

Magneto-optical studies of acceptors confined in GaAs/Al_xGa_{1-x}As quantum wells

P. O. Holtz, Q. X. Zhao, A. C. Ferreira, and B. Monemar

Departments of Physics and Mesasurement Technology, Linköping University, S-581 83 Linköping, Sweden

Alfredo Pasquarello

Institut Romand de Recherche Numérique en Physique des Matériaux (IRRMA), PHB-Ecublens, CH-1015 Lausanne, Switzerland

M. Sundaram, J. L. Merz, and A. C. Gossard

Center for Quantized Electronic Structures (QUEST), University of California at Santa Barbara, Santa Barbara, California 93106

(Received 23 November 1993; revised manuscript received 23 February 1994)

A magneto-optical study of acceptors in varying degrees of confinement in GaAs/Al_xGa_{1-x}As quantum wells (QW's) is presented. A model for the splitting of the acceptor bound exciton (BE) and the allowed BE transitions in the presence of a magnetic field is presented. Our experimental results for the acceptor BE emission agree with calculated g values for bound holes, e.g., $g_{3/2}=0.61$ and $g_{1/2}=0.35$ for a 150-Å-wide QW. Furthermore, the energy separation between the acceptor $m_j = \pm \frac{3}{2} 1S(\Gamma_6)$ ground state and the excited $m_j = \pm \frac{3}{2} 2S(\Gamma_6)$ state as a function of applied magnetic field is derived from selective photoluminescence and resonant-Raman-scattering measurements. Finally, these experimental results are compared with theoretical predictions for the confined acceptor states.

INTRODUCTION

While there are numerous reports on experimental studies of the effect of different external perturbations, such as electric, magnetic, and mechanical stress fields, on the intrinsic properties of quantum-well (QW) systems, corresponding studies on the extrinsic properties are very limited. For the case of the magnetic-field effect on confined donors, Jarosik *et al.*¹ performed work by using far-infrared (FIR) magnetospectroscopy. Later on, FIR magnetospectroscopic studies have resulted in several reports on, e.g., the dependence of the transition energies between the ground state and excited states on the QW width and the donor position within the QW for the Si donor confined in GaAs/Al_xGa_{1-x}As QW's.^{2,3} An alternative far-infrared technique to study the impurity transitions is the FIR photoconductivity method, which recently has been applied on the confined Si donor.^{4,5} For the case of acceptors, the energy levels for the excited states have been investigated as a function of QW width and acceptor position via resonant Raman scattering (RRS) and two-hole transitions (THT's) of the acceptor bound exciton (BE) observed in selective photoluminescence (SPL).^{6,7} Corresponding studies on the magnetic-field dependence of confined acceptors are very limited. Recently, there have been a few experimental reports on the g factor for the acceptor bound hole.⁸⁻¹⁰ For instance, Sapega *et al.* reported on spin-flip Raman scattering for the acceptor bound hole.⁹ From these measurements, the longitudinal component of the g factor for the acceptor bound hole could be evaluated, $g_{||}=2.3$, in a 40-Å-wide QW. These results deviate significantly from the theoretical treatment by Masselink, Chang, and Morkoç.¹¹ We have earlier reported on the confinement dependence of the effective g values for the acceptor BE recombination evaluated from magneto-optical measurements.¹² We have now extended these studies on the elec-

tronic structure of the acceptor and its BE on both the experimental and theoretical side. In this work we emphasize the experimental side, while the theoretical part is published separately.¹³

EXPERIMENT

The samples used in this study were grown by molecular beam epitaxy at a temperature of nominally 680°C without interruptions at the QW interfaces. On top of a semi-insulating (100) GaAs substrate, a 0.35- μ m undoped GaAs buffer layer and 50 periods of alternating layers of GaAs QW's of widths in the range 50–150 Å and 140-Å-wide Al_{0.30}Ga_{0.70}As barriers were grown. The samples were selectively doped with Be in the central 20% of the QW with a concentration ranging from $3 \times 10^{16} \text{ cm}^{-3}$ for the wide wells to $1 \times 10^{17} \text{ cm}^{-3}$ for the more narrow QW's.

For SPL and PL excitation measurements, an Ar⁺ ion laser was used to pump a titanium-doped sapphire solid-state laser. The emitted light from the samples was focused on the slits of a 1-m double-grating monochromator and detected with a dry-ice-cooled GaAs photomultiplier. The magneto-optical measurements have been performed in magnetic fields up to 16 T applied perpendicular to the QW layers. The excitation light from the laser is coupled onto the sample via an optical fiber. The same optical fiber is used for the collected emission light from the sample onto the monochromator.

LUMINESCENCE IN THE PRESENCE OF A MAGNETIC FIELD

While there are a number of papers on theoretical approaches to calculate the electronic structure of the confined acceptors without considering external-field perturbations, there is to the best of our knowledge only one earlier report by Masselink, Chang, and Morkoç¹¹ on the

theoretical treatment of the acceptor electronic structure in the presence of a magnetic field. They predicted the ground-state splitting between the acceptor Kramers doublet states, the $m_j = \pm \frac{3}{2}$ states; however, the predicted splitting was significantly larger than the experimental results reported.^{8–10}

Recently, we have performed calculations on the energy levels for acceptor states perturbed by a magnetic field by extending the comprehensive theory given by Fraizzoli and Pasquarello.^{14,15} The acceptor states are calculated within a four-band effective-mass theory, in which the valence-band mixing as well as the mismatch of the valence-band parameters and the dielectric constants between well and barrier materials have been taken into account. To ensure that the calculations converge for all different states, a large number of basis functions (up to 1000) have been used. The g factors of shallow acceptor states are obtained from these calculations for varying QW widths and for different input values on the Luttinger parameters, κ and q . The details about the calculations performed are given elsewhere.¹³

PL spectra of QW structures at moderate acceptor doping levels are normally dominated by the free exciton and the acceptor BE. In the presence of a magnetic field, the acceptor BE peak is blueshifted due to the diamagnetic shift (measures to 2.1×10^{-2} meV/T² for a 150-Å-wide QW). Furthermore, the BE peak is found to split into two components in magnetic-field-perturbed PL.¹² One has to proceed cautiously, however, when interpreting this linear Zeeman splitting. In the presence of a magnetic field, not only the twofold degeneracies of the ground states [the $1S(\Gamma_6)$ heavy-hole state and the $1S(\Gamma_7)$ light-hole state] are lifted, but also the excited acceptor BE states split. Consequently, the observed splitting of the acceptor BE peak as observed in PL spectra is the combined effect of the splitting in the acceptor ground state and the excited acceptor BE state. Accordingly, the g values, for the electron and hole individually cannot be directly determined from these spectra, but instead an effective g value, g_{eff} , for the entire acceptor BE emission is evaluated. The so-derived effective g value is found to be significantly larger for an acceptor BE confined in a QW than in bulk material. For instance, the acceptor BE effective g value is reduced from $g_{\text{eff}} = 1.89$ for a 100-Å-wide QW to $g_{\text{eff}} = 0.66$ for the corresponding BE emission in bulk GaAs.¹²

In order to further proceed with the interpretation of the magneto-optical results achieved, we have to treat the electronic structure of the acceptor ground state and the excited acceptor BE state separately. If we start with the acceptor $1S(\Gamma_6)$ ground state, the linear magnetic-field splitting between the acceptor $\pm |J_z|$ components can be described by

$$\Delta E = \mu_B g_{J_z} 2 |J_z| B,$$

where J_z is the magnetic angular momentum in the direction of the magnetic field and g_{J_z} is the related g value. The g values for the confined acceptor holes have recently been calculated,¹³ and are found to be in good agreement with the independent experimental data available.^{8–10}

The so-derived splitting for the acceptor $1S(\Gamma_6)$ ground state, i.e., the final state in the PL emission, in a 150-Å-wide QW for a g value of $g_{3/2} = 0.61$ and $g_{1/2} = 0.35$ (Ref. 13) is shown in Fig. 1.

We now proceed with the initial state in the PL emission, the acceptor BE state. The j - j coupling between the two bound holes and the single electron involved in the BE system gives rise to three BE states with $J = \frac{1}{2}, \frac{3}{2},$ and $\frac{5}{2}$, of which the $J = \frac{5}{2}$ BE state is concluded to be lowest for shallow acceptor BE's in bulk GaAs (Ref. 16) as well as in QW's.¹² Also, the QW confinement effect has to be considered in a proper treatment of the BE in the two-dimensional case. This confinement effect, included in the calculations via the introduction of an axial crystal-field perturbation, results in a further splitting of the BE states. This splitting is, however, concluded to be significantly smaller than the splitting between the $J = \frac{3}{2}$ and $\frac{5}{2}$ BE states (by more than a factor of 10) (Ref. 12) and is, accordingly, below our resolution limit.

We can now conclude our discussion on the BE emission by stating that the transition observed in PL at low temperatures originates from the initial $J = \frac{5}{2}$ acceptor BE state to the final acceptor $1S(\Gamma_6)$ ground state. The calculated dependence of these states on the magnetic field together with the allowed transitions are shown in Fig. 1. The solid lines show the σ -polarized transitions, while the dashed lines show the π -polarized transitions, which are forbidden in the Faraday configuration used in

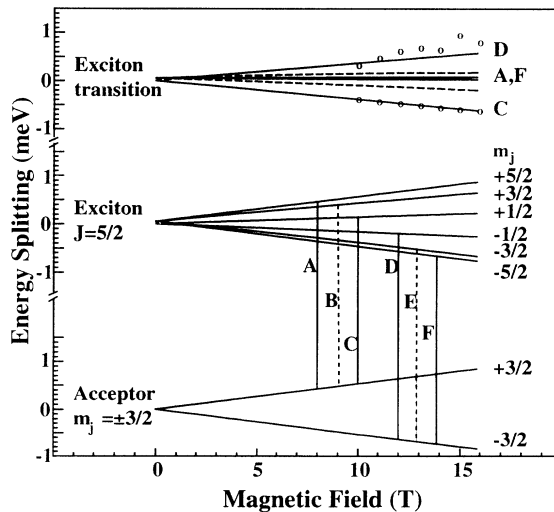


FIG. 1. The predicted development of partly the acceptor $m_j = \pm \frac{3}{2}$ $1S(\Gamma_6)$ ground-state components and partly the $J = \frac{5}{2}$ BE-state components, with increasing magnetic field, for a 150-Å QW is shown in the lower part of this figure. The allowed transitions between these components (denoted A–F) are given by solid lines corresponding to the σ -polarized transitions and dashed lines for the π -polarized transitions (forbidden in our Faraday configuration). The resulting splitting for the allowed transitions between the BE state and the $1S(\Gamma_6)$ ground state of the acceptor as a function of the magnetic field is shown in the top part of this figure. In order to compare with experimental results, the splitting of the acceptor BE observed in PL measurements is plotted relative to the low-energy branch (denoted C).

this experiment. The resulting splitting for the allowed transitions between the BE state and the $1S(\Gamma_6)$ ground state of the acceptor, as a function of the magnetic field, is shown in the top part of Fig. 1. For comparison, the experimentally observed splitting of the BE peak relative to the low-energy branch (*C*) is shown in the same figure. The derived PL results agree within the experimental accuracy with the predicted exciton transitions for the low-energy and high-energy branches (denoted *C* and *D* in Fig. 1), while the two remaining components (*A* and *F* in Fig. 1) have not been monitored in our PL spectra. These components might be hidden between the *C* and *D* components due to a somewhat smaller transition probability for *A* and *F*.

MAGNETIC-FIELD DEPENDENCE OF ACCEPTOR STATES

The acceptor $1S(\Gamma_6)$ - $2S(\Gamma_6)$ energy separation has been measured as a function of the applied magnetic field in two independent ways: the separation between the acceptor BE peak and the dominating THT satellite related to the excited $2S(\Gamma_6)$ acceptor state or, alternatively, the separation between the laser excitation energy and the strongest RRS satellite. The results derived from these two methods are almost identical, but since the experimental accuracy is significantly higher for the case of the RRS, the results we refer to in this paper originate from RRS. The satellite peaks are found to shift towards higher energy with increasing magnetic field like the acceptor BE's, but at a slightly slower rate than the BE's. This means that the energy separation between the acceptor BE's and the THT satellites, i.e., the $1S(\Gamma_6)$ - $2S(\Gamma_6)$ (Fig. 2) transition energy, increases with increasing magnetic field. The same trend is found for all QW widths investigated, although to a different extent. The dependence of the acceptor $1S(\Gamma_6)$ - $2S(\Gamma_6)$ transition energy on the applied magnetic field up to 16 T for three different QW widths is shown in Fig. 3.

The experimentally achieved results on the energy sep-

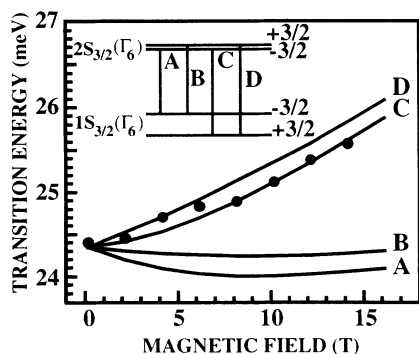


FIG. 2. The inset shows schematically the splitting of the $m_j = \pm \frac{3}{2}$ components for the $1S(\Gamma_6)$ ground state and the $2S(\Gamma_6)$ excited state of the confined acceptor in the presence of a magnetic field. The possible transitions between the acceptor $1S(\Gamma_6)$ ground state and $2S(\Gamma_6)$ excited state are denoted by *A*–*D*. The main figure shows the calculated transition energies for the case of an acceptor in the center of a 100-Å-wide QW. The experimental results derived from the RRS and THT experiments are given as filled circles in the figure.

aration between the acceptor $1S(\Gamma_6)$ ground state and the excited $2S(\Gamma_6)$ state have been compared with theoretically predicted results. From the computations described above, the dependence for different acceptor states on the applied magnetic field has been calculated. The inset in Fig. 2 shows schematically the energy levels for the acceptor $1S(\Gamma_6)$ ground state and the excited $2S(\Gamma_6)$ state in the presence of a magnetic field. The energy levels resulting from these calculations for the acceptor $1S(\Gamma_6)$ ground state and the excited $2S(\Gamma_6)$ state are shown in Fig. 2 for the case of acceptors in the center of a 100-Å-wide QW. As can be seen in this figure, the predicted splitting between the Kramers doublet states, the $m_j = \pm \frac{3}{2}$ states, is significantly larger for the $1S(\Gamma_6)$ ground state than for the excited $2S(\Gamma_6)$ state. There are four possible transitions between the acceptor $1S(\Gamma_6)$ ground state and the excited $2S(\Gamma_6)$ state, denoted *A*, *B*, *C*, and *D* in Fig. 2, of which two transitions $m_j = \pm \frac{3}{2} \leftrightarrow m_j = \mp \frac{3}{2}$ involve a spin flip.⁹ Since the splitting between the $m_j = \pm \frac{3}{2}$ components of the $2S(\Gamma_6)$ excited state is small relative to the corresponding splitting of the $1S(\Gamma_6)$ ground state, we derive two major branches [related to $m_j = +\frac{3}{2}$ and $-\frac{3}{2}$, respectively, of the $1S(\Gamma_6)$ ground state] of predicted transition energies for central acceptors in a 100-Å-wide QW, as shown in Fig. 2.

Next we will compare the experimental results achieved with the theoretical predictions for the acceptor $1S(\Gamma_6)$ - $2S(\Gamma_6)$ transition energy in a 150-Å-wide QW shown in Fig. 2. First, we will state that the resolution of the experiments does not allow us to draw any conclusions about whether the spin-conserving, $m_j = \pm \frac{3}{2} \leftrightarrow m_j = \pm \frac{3}{2}$ or the spin-flip, $m_j = \pm \frac{3}{2} \leftrightarrow m_j = \mp \frac{3}{2}$, transitions dominate between the acceptor $1S(\Gamma_6)$ - $2S(\Gamma_6)$ states. Second, we note that just one branch corresponding to the high-energy branch is observed, while the low-energy branch is not seen. The reason for the absence of this branch is obscure, but it should be kept in mind that the experimental results originate from measurements of RRS or THT satellites with resonant excitation, and the selection rules applicable to RRS or THT have to be taken into account. Possible explanations for the absence or low intensity of the low-energy branch are a low oscillator strength for RRS or THT transitions re-

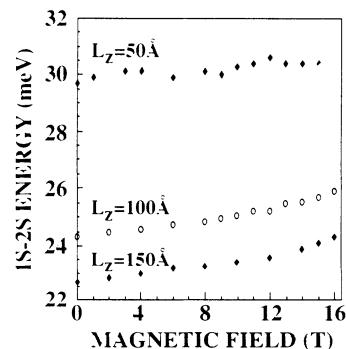


FIG. 3. The experimentally determined energy separation between the acceptor $1S(\Gamma_6)$ ground state and the excited $2S(\Gamma_6)$ state as a function of applied magnetic field for three different QW widths.

lated to this branch or a limited thermal population of the initial BE state. However, the experimental data for the high-energy branch for the acceptor $1S(\Gamma_6)$ - $2S(\Gamma_6)$ transition energy exhibit a good agreement with the theoretical predictions, when the Luttinger parameter $\kappa = 1.2$ is used.¹³

SUMMARY

In summary, we have performed optical studies of the acceptor confined in $\text{GaAs}/\text{Al}_x\text{Ga}_{1-x}\text{As}$ quantum wells

of varying width in the presence of a magnetic field. The magnetic-field dependence of the transitions between the acceptor $1S(\Gamma_6)$ ground state and the excited $2S(\Gamma_6)$ state is demonstrated. Also, a model for the magnetic-field dependence of the acceptor BE recombination from the initial $J = \frac{5}{2}$ BE state to the final $1S(\Gamma_6)$ acceptor ground state is presented. The experimental data on the acceptor BE splitting observed in PL as a function of magnetic field are in good agreement with our results from calculations on bound-hole g values.

-
- ¹N. C. Jarosik, B. D. McCombe, B. V. Shanabrook, and J. Comas, *Phys. Rev. Lett.* **54**, 1283 (1985).
²J.-M. Mercy, Y.-H. Chang, A. A. Reeder, G. Brozak, and B. D. McCombe, *Superlatt. Microstruct.* **4**, 213 (1988).
³S. Huant, R. Stepniewski, G. Martinez, V. Thierry-Mieg, and B. Etienne, *Superlatt. Microstruct.* **5**, 331 (1989).
⁴J.-P. Cheng and B. D. McCombe, *Phys. Rev. B* **42**, 7626 (1990).
⁵J. L. Dunn, E. Pearl, R. T. Grimes, M. B. Stanaway, and J. M. Chamberlain, *Mater. Sci. Forum* **65-66**, 117 (1990).
⁶P. O. Holtz, M. Sundaram, K. Doughty, J. L. Merz, and A. C. Gossard, *Phys. Rev. B* **40**, 12 338 (1989).
⁷G. C. Rune, P. O. Holtz, B. Monemar, M. Sundaram, J. L. Merz, and A. C. Gossard, *Phys. Rev. B* **44**, 4010 (1991).
⁸H. W. van Kesteren, E. C. Cosman, W. A. J. A. van der Pole, and C. T. Foxon, *Phys. Rev. B* **41**, 5283 (1990).
⁹V. F. Sapega, M. Cardona, K. Ploog, E. L. Ivchenko, and D. N. Mirlin, *Phys. Rev. B* **45**, 4320 (1992).
¹⁰D. N. Mirlin and A. A. Sirenko, *Fiz. Tverd. Tela (Leningrad)* **34**, 205 (1992) [*Sov. Phys. Solid State* **34**, 108 (1992)].
¹¹W. T. Masselink, Y. C. Chang, and H. Morkoç, *Phys. Rev. B* **32**, 5190 (1985).
¹²P. O. Holtz, Q. X. Zhao, B. Monemar, M. Sundaram, J. L. Merz, and A. C. Gossard, *Phys. Rev. B* **47**, 15 675 (1993).
¹³Q. X. Zhao, P. O. Holtz, A. Pasquarello, B. Monemar, A. C. Ferreira, M. Sundaram, J. L. Merz, and A. C. Gossard, *Phys. Rev. B* **49**, 10 794 (1994).
¹⁴S. Fraizzoli and A. Pasquarello, *Phys. Rev. B* **42**, 5349 (1990).
¹⁵S. Fraizzoli and A. Pasquarello, *Phys. Rev. B* **44**, 1118 (1991).
¹⁶A. M. White, P. J. Dean, and B. Day, *J. Phys. C* **7**, 1400 (1974).